ENGINEERING JOURNAL

Article

Two-Dimensional Modeling of the Oxidative Coupling of Methane in a Fixed Bed Reactor: A Comparison among Different Catalysts

Salamah Manundawee[1], Amornchai Arpornwichanop[2], Suttichai Assabumrungrat[2], and Wisitsree Wiyaratn[1,*]

1 Faculty of Industrial Education and Technology, King Mongkut's University of Technology Thonburi, Bangkok 10140, Thailand
2 Department of Chemical Engineering, Faculty of Engineering, Chulalongkorn University, Bangkok 10330, Thailand

*E-mail: wisitsree.wiy@kmutt.ac.th (Corresponding author)

Abstract. A proposed two-dimensional model of the oxidative coupling of methane (OCM) to C_2 hydrocarbons (e.g., C_2H_4 and C_2H_6) in a fixed bed reactor operated under isothermal and non-isothermal conditions is described which can provide more accurate predictions of experimental data than the simplified one-dimensional model. The model includes a set of partial differential equations of the continuity, mass transfer and energy balance equations. The performance of the OCM using different catalysts was assessed in terms of CH_4 conversion, C_2 selectivity and C_2 yield with respect to key operating parameters, such as feed temperature (973-1173 K), CH_4/O_2 ratio (3.4–7.5) and gas hour space velocity (GHSV) (18000-30000 h^{-1}). The simulation results indicated that the Na-W-Mn/SiO_2 catalyst exhibits the best performance among all of the catalysts. The C_2 yield were 20.16% and 20.00% for non-isothermal and isothermal modes respectively which the OCM reactor is operated at a CH_4/O_2 ratio of 3.4, a feed temperature of 1073 K and a GHSV of 9720 h^{-1}. An increase in the operating temperature increases the CH_4 conversion but decreases the C_2 selectivity. However, the effects of the CH_4/O_2 ratio and the GHSV exhibit an opposite trend to that of the operating temperature.

Keywords: Oxidative coupling of methane (OCM), fixed bed reactor, two-dimensional model, gas hour space velocity (GHSV).

ENGINEERING JOURNAL Volume 21 Issue 3
Received 24 June 2016
Accepted 6 December 2016
Published 15 June 2017
Online at http://www.engj.org/
DOI:10.4186/ej.2017.21.3.77

DOI:10.4186/ej.2017.21.3.77

1. Introduction

Natural gas consists primarily of methane and is a raw material for a number of synthetic products [1]. One of many processes for natural gas utilization is oxidative coupling of methane (OCM); this process can directly convert methane into precious C_2 hydrocarbons. Works on the OCM reaction have been reported since the pioneering work of Keller and Bhasin in 1982. However, it is still a great challenge to improve on obtaining higher conversion of methane and ethylene, and high C_2 hydrocarbons selectivity in the production process [2].

In OCM process, several reactions occur simultaneously including homogeneous gas phase reactions and heterogeneous catalytic reactions, parallel and consecutive reaction with very complex reaction kinetics. Numerous kinetic reaction models have been presented to describe the performance of the OCM process over a large number of catalysts [3-7]. Several catalysts for OCM reaction were found to be effective in heterogeneous–homogeneous complex process [8] . Parameters of metal oxides, such as basicity, band gap, and electrical oxidative coupling of methane conductivity were some of the important parameters in affecting the catalyst performance. However, Li/MgO, La_2O_3/CaO and Na-W-Mn/SiO_2 were three of the most popular catalysts presented in the literature involving the studies of the OCM process because of their high performance [9-13]. Li/MgO is one of the most commonly studied OCM catalyst system, particularly to show that higher C_2 yields (> 70%) are attained in the dense oxide membrane reactor than in conventional packed-bed reactors and it showed high catalytic activity in the low temperature range [14-16]. In additional, La_2O_3/CaO demonstrated a promising result with 42% methane conversion and yield up to 20% [17]. Their kinetic reaction for OCM has been a strong interest in Na-W-Mn/SiO_2 and is thus extensively studied by several researchers. Their experimental results suggested this catalyst had appealing prospects in commercial application [18].

There are many types of reactors such as moving bed chromatographic reactor, membrane reactor, fluidized-bed reactor, catalytic jet-stirred reactor, and fixed bed reactor, have been reported. The applications of membrane reactor combining the separation and reaction in one unit to control oxygen concentration along the reactor were promising in enhancing CH_4 conversion, yield and C_2 selectivity for OCM process. The performances of catalytic membrane reactor (CMR), catalyst packed bed membrane reactor (PBMR), and packed bed reactor (PBR) were compared at optimum condition and found that CMR performed best among three reactors with CH_4 conversion by Bhatia and his co-workers [19]. Wang and co-workers showed the remarkable study that the improvement of C_2 selectivity was observed when catalyst was packed in the membrane tube [20]. Fixed bed reactor is investigated in the most studied due to technically feasible and economic. Using mathematical model in fixed bed reactor study on OCM process was the easiest to design, scale up, and could be analyzed. In addition, OCM is an extremely exothermic reaction, and hot spots always occur in the catalyst. Heat removal was therefore essential for practical operation, and reactors were likely to be operated under non-isothermal condition [21]. The design of the fixed bed reactor using a two-dimensional mathematical model considering both axial- and radial-directions is more complex than that of a one-dimensional study considering only the axial axis. The two-dimensional model is more realistic and provides better prediction accuracy than the one-dimensional model. The need for the two-dimensional model becomes essential when a reactor with a large diameter is operated because the effect of radial dispersion becomes more pronounced. In the reactor design, it is important to determine a location where the hot spot is severe so that the operational problems, such as catalyst sintering, can be avoided and a suitable operating condition can be selected.

Therefore, in this study, two-dimensional mathematical modelling of the oxidative coupling of methane (OCM) to C_2 hydrocarbons (C_2H_4 and C_2H_6) in a fixed bed operated under isothermal and non-isothermal conditions is investigated using the COMSOL® Multiphysics Program. Fixed bed reactors are modelled using the available information on the reaction kinetics of three different catalysts. The simulations are aimed at finding a suitable catalyst and determining the performance of the OCM process using a two-dimensional mathematical model.

2. Simulation

2.1. Kinetic Model

Numerous kinetic reaction models have been presented to describe the performance of the OCM process over several catalysts. Li/MgO, La_2O_3/CaO and Na-W-Mn/SiO_2 are three of the most studied catalysts in the literature related to the OCM process. Li/MgO exhibits high catalytic activity in the low temperature range, La_2O_3/CaO was one of the most common catalysts used in OCM models and Na-W-Mn/SiO_2 was one of the most studied three-component catalyst. In the model, the kinetic mechanism and kinetic equations considered in this work were proposed by Wang and Lin [3] over a Li/MgO catalyst, Stansch et al. [4] over a La_2O_3/CaO catalyst and Danespayeh et al. [18] over a Na-W-Mn/SiO_2 catalyst. The stoichiometric equation and reaction rate of each of the proposed models are presented in Table 1.

2.2. Reactor Model

The transport phenomena were coupled with the reaction kinetics to develop a reactor model. The two-dimensional flow field in a fixed bed reactor was coupled with the mass and heat transport for the simulation performance of the OCM process, as well as the velocity, concentration and temperature profiles.

2.2.1. Geometry and boundary condition

The reactor geometry considered was a 2D cylindrical one, and the flow enters the computational domain at a known velocity, composition and temperature. At the outlet, it was assumed that the convective part of the mass and heat transport vector was dominating. At the tube wall, a heat transfer was defined in non-isothermal mode, which defined the wall insulation in adiabatic operation, and the heat flux was removed from the wall in constant-wall temperature operation. The geometry of the fixed bed reactor is presented in Figure 1, which shows the scheme of the FBR. Methane and air were mixed and co-fed to an impermeable tubular reactor; the inner tube was filled with a bed of catalyst.

The reactor model was based on the following basic assumptions: two-dimensional mathematical model, steady-state operation and ideal gas behaviour. In addition, diffusivity in the catalyst bed was assumed to be via the Knudsen mechanism.

2.2.2. Governing equations

Mass balance: the mass balance for each of the eight components can be written as

$$\left(\frac{\partial^2 C_i}{\partial r^2} + \frac{1}{2}\frac{\partial C_i}{\partial r}\right) + D_i \frac{\partial^2 C_i}{\partial z^2} - u\frac{\partial C_i}{\partial z} + \rho_B r_i = 0 \quad (1)$$

The rate of production was calculated for each component from the stoichiometry of the reactions.

Energy balance: the energy balance for the reactor can be written as follows.

$$\lambda\left(\frac{\partial^2 T}{\partial r^2} + \frac{1}{2}\frac{\partial T}{\partial r}\right) + \frac{\partial^2 T}{\partial z^2} - u\rho_f C_p \frac{\partial T}{\partial z} + Q = 0 \quad (2)$$

The heat source in Eq. (2), including heat of reaction and heat flux, were computed by

$$Q = \sum_{i=1}^{n} \Delta H_{rxn} r_i + U(T - T_{ex}) \quad (3)$$

Momentum balance: the momentum balance for reactor describes the flow in the porous media. The equation extends Darcy's law combination with the continuity equation:

$$\nabla\left(-\eta(\nabla u + (\nabla u)^T)\right) + \frac{k}{\eta}u = 0 \quad (4)$$

DOI:10.4186/ej.2017.21.3.77

Table 1. Stoichiometric equation and reaction rate of proposed models.

Model	Stoichiometry equation	Reaction rate
Wang and Lin	Step 1 : $CH_4+2O_2 \rightarrow CO_2+2H_2O$ Step 2 : $2CH_4+0.5O_2 \rightarrow C_2H_6+H_2O$ Kinetic parameters: $K_1 = 2.472 \times 10^7 e^{-49.649/RT}$ $K_2 = 10.10e^{-23.15/RT}$ $K_3 = 0.103 \times 10^{-3} e^{-4.548/RT}$ $K_4 = 0.093 \times 10^{-4} e^{27.94/RT}$	$r_1 = \frac{K_3 P_{O_2}^{1.251}}{4}\left[\left(1+\frac{8K_2\frac{C_p}{C_T}P_{CH_4}}{K_3P_{O_2}^{1.251}}\right)^{0.5}-1\right]+16S_0K_2\frac{C_p}{C_T}P_{C_2}$ $r_1 = \frac{K_3 P_{O_2}^{1.251}}{16}\left[\left(1+\frac{8K_2\frac{C_p}{C_T}P_{CH_4}}{K_3P_{O_2}^{1.251}}\right)^{0.5}-1\right]^2+8S_0K_2\frac{C_p}{C_T}P_{C_2}$ $\frac{C_p}{C_T} = \frac{K_1P_{O_2}^{0.5}}{K_1P_{O_2}^{0.5}+K_1K_2K_4+K_2(P_{CH_4}+8S_0P_{C_2})}$ $S_0 = \frac{2}{\left(1+\frac{8K_2\frac{C_p}{C_T}P_{CH_4}}{K_3P_{O_2}^{1.251}}\right)^{0.5}+1}$ $Z = \frac{K_1P_{O_2}^{0.5}}{K_1P_{O_2}^{0.5}+K_1K_2K_4+K_2(P_{CH_4}+8S_0P_{C_2})}$
Stansch *et al.*	Step 1 : $CH_4+2O_2 \rightarrow CO_2+2H_2O$ Step 2 : $2CH_4+0.5O_2 \rightarrow C_2H_6+H_2O$ Step 3 : $CH_4+O_2 \rightarrow CO+H_2O+H_2$ Step 4 : $CO+0.5O_2 \rightarrow CO_2$ Step 5 : $C_2H_6+0.5O_2 \rightarrow C_2H_4+H_2O$ Step 6 : $C_2H_4+2O_2 \rightarrow 2CO+2H_2O$	$r_j = \frac{k_{0j}e^{-\frac{E_{0,j}}{RT}}P_C^{m_j}P_{O_2}^{n_j}}{\left(1+K_{jCO_2}e^{-\Delta H_{od,O_2/RT}}P_{CO_2}\right)^2} \quad j = 1,3-6$

DOI:10.4186/ej.2017.21.3.77

Model	Stoichiometry equation	Reaction rate
	Step 7 :C_2H_6 → $C_2H_4+H_2$ Step 8 :$C_2H_4+2H_2O$ → $2CO+2H_2O$ Step 9 :$CO+H_2O$ → CO_2+H_2 Step 10 :CO_2+H_2 → $CO+H_2O$	$r_2 = \frac{k_{02}e^{\frac{-E_2}{RT}}(K_{0O_2}e^{-\Delta H_{od,O_2/RT}}P_{O_2})^{n_1}P_{CH_4}}{[1+(K_{0O_2}e^{-\Delta H_{od,O_2/RT}}P_{O_2})^{n_1}+K_{0O_2}e^{-\Delta H_{od,O_2/RT}}P_{O_2}]^2}$ $r_7 = k_{07}e^{-E/RT}P_{C_2H_6}^{m_7}$, $r_8 = k_8e^{-E/RT}P_{C_2H_6}^{m_8}P_{H_2O}^{n_8}$ $r_9 = k_{09}e^{-E/RT}P_{CO_2}^{m_9}P_{H_2}^{n_9}$, $r_{10} = k_{10}e^{-E/RT}P_{CO}^{m_{10}}P_{H_2O}^{n_{10}}$
Danespayeh *et al.*	Step 1 : $2CH_4+0.5O_2$ → $C_2H_6+H_2O$ Step 2 : CH_4+2O_2 → CO_2+H_2O Step 3 :CH_4+O_2 → $CO+H_2O+H_2$ Step 4 :$CO+0.5O_2$ → CO_2 Step 5 :$C_2H_6+0.5O_2$ → $C_2H_4+H_2O$ Step 6 :$C_2H_4+2O_2$ → $2CO+2H_2O$ Step 7 :$C_2H_4+2H_2O$ → $2CO+4H_2$ Step 8 :C_2H_6 → $C_2H_4+H_2$ Step 9 :CO_2+H_2 → $CO+H_2O$ Step 10 :$CO+H_2O$ → CO_2+H_2	$r_1 = \frac{k_{01}e^{\frac{-E_1}{RT}}(K_{0O_2}e^{-\Delta H_{od,O_2/RT}}P_{O_2})^{n_1}P_{CH4}^{m2}}{[1+(K_{0O_2}e^{-\Delta H_{od,O_2/RT}}P_{O_2})^{n_1}]^2}$ $r_j = k_{0j}e^{-E/RT}P_C^{m_j}P_{O_2}^{n_j} \quad j = 2-6$ $r_7 = k_{07}e^{-E/RT}P_{C_2H_4}^{m_7}P_{H_2O}^{n_j}$, $r_8 = k_{08}e^{-E/RT}P_{C_2H_6}^{m_8}$ $r_9 = k_{09}e^{-E/RT}P_{CO_2}^{m_9}P_{H_2}^{n_9}$, $r_{10} = k_{10}e^{-E/RT}P_{CO}^{m_{10}}P_{H_2O}^{n_{10}}$

The performance of the reactor was evaluated by the conversion of reactants as well as the selectivity and the yield of the products. The conversion was defined as the fraction of the reactant that was reacted to the amount of reactant fed. For example, the conversion of methane was

$$CH_4 \text{ conversion } \% = \frac{F^0_{CH_4} - F_{CH_4}}{F^0_{CH_4}} \times 100 \quad (5)$$

and the C_2 selectivity was defined as the C_2 product formed per reactant consumed.

$$C_2 \text{ selectivity } \% = \frac{2\times(F_{C2H4}+F_{C2H6})}{(2(F_{C2H4}+F_{C2H6})+F_{CO}+F_{CO2})} \times 100 \quad (6)$$

Moreover, the CO_x selectivity was defined as the CO_x byproduct formed per reactant consumed.

$$CO_x \text{ selectivity } \% = \frac{F_{CO}+F_{CO2}}{(2(F_{C2H4}+F_{C2H6})+F_{CO}+F_{CO2})} \times 100 \quad (7)$$

The yield referred to the specific product formed per reactant fed.

$$C_2 \text{ yield } \% = \frac{2\times(F_{C2H4}+F_{C2H6})}{F^0_{CH_4}} \times 100 \quad (8)$$

In addition, in a fixed bed reactor, the effect of operating variables under three operating modes, i.e., isothermal, adiabatic, and non-isothermal condition, were considered.

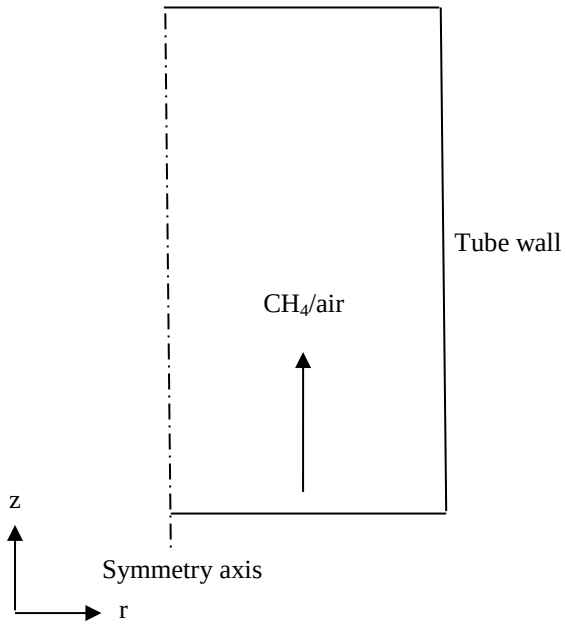

Fig. 1. Geometry of fixed bed reactor.

2.3. Numerical Approach

The finite element method was proposed to formulate the PDE problem. In the developed finite element model, the reactor was solved with quadratic finite element basis functions using the commercial finite element simulation environment COMSOL. The software runs the finite element analysis together with meshing, which involves a partition of the geometry model into small units of simple shapes, and error control using a variety of numerical solvers. Three application modes were required to model the heat transfer by conductive and convective processes. Mass transfer by convective processes and diffusion was

used to simulate the concentration and transport of eight species of interest. The Brinkman equation was applied to describe the fluid flow.

3. Results and Discussion

The simulations were performed for OCM in a fixed bed reactor. The conditions used in the simulation are summarized in Table 2, and the catalyst properties are presented in Table 3.

Table 2. Reactor dimension and conditions.

Condition	Dimension
Fixed bed reactor	
Length of catalyst bed (m)	0.2
Diameter (m)	0.018
Temperature (K)	993-1173
Pressure (kPa)	101.325
CH_4/O_2 ratio	3.4-7.5
GHSV (h^{-1})	18000-30000

Table 3. Catalyst properties.

Property	**catalyst**		
	Li/MgO	La_2O_3/CaO	Na-W-Mn/SiO_2
Average pore radius (m)	0.0005	0.01	0.00008
Porosity (-)	0.34	0.6	0.6
Totousity (-)	2.153	3	1.089
Thermal conductivity (W/m K)	10.3	1	1.35

3.1. Model Validation

The validation of the kinetic model (for Li/MgO, La_2O_3/CaO and Na-W-Mn/SiO_2 catalyst) was performed first to ensure that the mathematical models could well predict the OCM performances. The model used was the two-dimensional plug flow model.

The validity of the Li/MgO catalyst using the kinetic rate expression reported by Wang and Lin [3] was assessed by comparing our simulation results with the simulation data from the literature [13] in the fixed bed reactor. Figure 2(a) shows yield of the C_2 products versus the run numbers under the conditions in the literature, which are presented in Table 4(a). Figure 2(b) shows the validation results of the La_2O_3/CaO catalyst by comparing our simulation results with the simulation data reported by Tye et al. [12] in terms of the C_2 yield versus the run numbers under the conditions of the literature, which are presented in Table 4 (b). Figure 2(c) shows the comparison between our results and the results reported in the literature by Daneshpayeh et al. [18] for a Na-W-Mn/SiO_2 catalyst, which provided conversion of CH_4 in a range of 16.5 – 19 kg m^3/s at a temperature of 1048 K. Our simulation results are found to agree well with simulation data from the literature.

DOI:10.4186/ej.2017.21.3.77

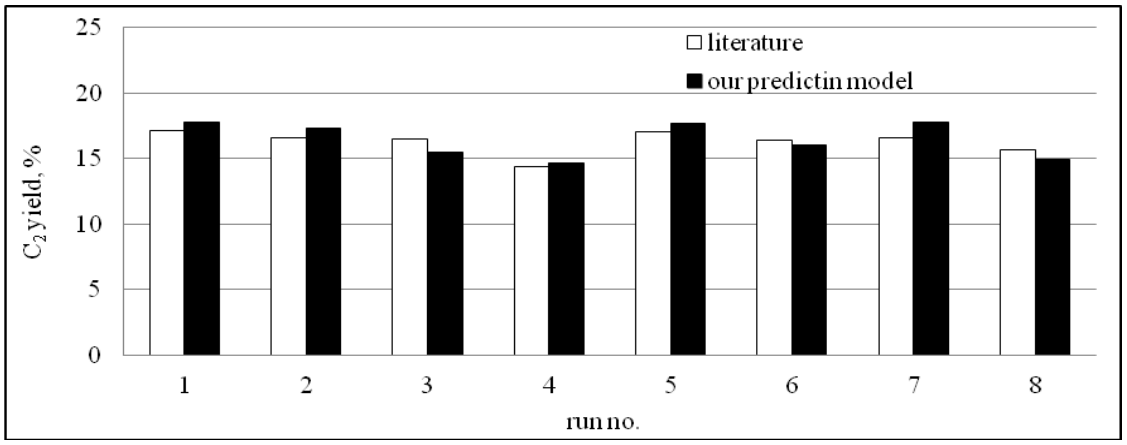

(a)

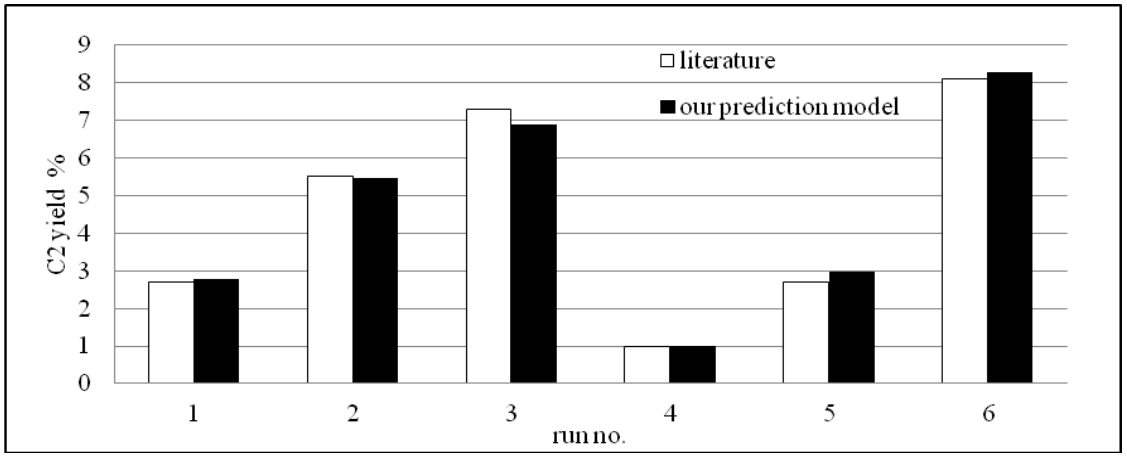

(b)

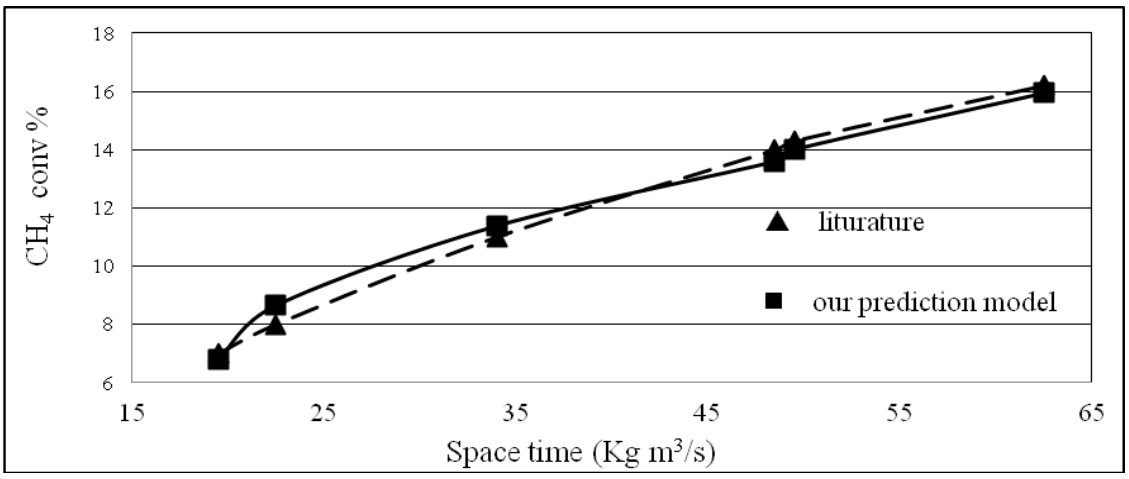

(c)

Fig. 2. Comparison between literature and our prediction model over Li/MgO (a.), La_2O_3/CaO (b.) and Na-W-Mn/SiO_2 (c.) catalysts.

Table 4. Condition for different run number.

Model	Condition	Run no.							
		1	2	3	4	5	6	7	8
(a) Kao *et al.* (1997)	Temperature(K)	993							
	Feed flow rate (mL/s)	0.83							
	Feed composition								
	- He	0.8921	0.8566	0.7882	0.3347	0.8842	0.8763	0.8447	0.5592
	- CH_4	0.0724	0.1118	0.1118	0.3987	0.0776	0.0763	0.1171	0.2868
	- O_2	0.0355	0.0316	0.1000	0.2066	0.0382	0.0474	0.0382	0.1540
(b) Tye *et al.* (2002)	Temperature (K)	1023	1073	1103	973	1023	1103		
	Feed flow rate (mL/s)	4							
	Feed molar ratio								
	- CH_4	0.612	0.612	0.612	0.699	0.699	0.699		
	- O_2	0.051	0.051	0.051	0.095	0.095	0.095		
	- N_2	0.337	0.337	0.337	0.206	0.206	0.206		

3.2. Catalytst Selection

This section considers the selection of a suitable catalyst among Li/MgO, La_2O_3/CaO and Na-W-Mn/SiO_2 catalysts at various conditions, i.e., gas hourly space velocity (GHSV), CH_4/O_2 ratio, and temperature. The system was based on a fixed bed reactor under isothermal operation mode. A summary of the operating conditions in this section is presented in Table 5.

The performance of the OCM reaction was considered in terms of the CH_4 conversion and the C_2 selectivity. Figure 3 shows the activities of the three catalysts for GHSV in a range of 18000 to 30000 1/h. The order of the CH_4 conversion follows Na-W-Mn/SiO_2 > La_2O_3/CaO > Li/MgO. The CH_4 conversion was decreased with the increase of the GHSV for all catalysts.

Figures 4-8 show the results of the C_2 selectivity to CH_4 conversion at a position of reactor length (the inlet of the reactor at CH_4 conversion was set to zero) under different conditions, which are summarized in Table 5 from all figures; the CH_4 conversion was increased and the C_2 selectivity was decreased with an increase of the distance from the inlet to the reactor for all catalysts. It was obvious that CH_4 conversion for the Na-W-Mn/SiO_2 catalyst was higher than those for the La_2O_3/CaO and Li/MgO catalysts. Moreover, the C_2 selectivity for the Na-W-Mn/SiO_2 catalyst was higher than those for the Li/MgO and La_2O_3/CaO catalysts. The CO_x selectivity for the La_2O_3/CaO catalyst was higher than those for the Li/MgO and Na-W-Mn/SiO_2 catalysts at all conditions. In addition, even the La_2O_3/CaO catalyst provides a CH_4 conversion higher than that of the Li/MgO catalyst, but the C_2 selectivity was lower. The presence of oxygen as a co-feed reactant affected to limited CH_4 conversion at different values as a result of consumed oxygen completely in the reaction. The comparison of the OCM performance among the catalysts at various CH_4/O_2 ratios is shown in Figs. 4-6. The CH_4 conversion was decreased while the C_2 selectivity was increased with the increase of the CH_4/O_2 ratio for all catalysts. Moreover, the comparison of the OCM performance among the different catalysts at various temperatures is shown in Figs. 6-8. The CH_4 conversion increased and the C_2 selectivity decreased with an increase of the temperature. Note that at higher temperature, the rate of decrease of the C_2 selectivity was greater than that at lower temperature, for example, for the Li/MgO catalyst, at 1173 K, the difference of C_2 selectivity between the outlets to the inlet was 4.43 % but at 993 K and 1073 K, the differences were 3.58 % and 3.84 %, respectively. The maximum C_2 yields for all catalysts at a temperature of 1173 K and a CH_4/O_2 ratio of 3.4 were 30.07 %, 19.2 % and 20.43 % for Na-W-Mn/SiO_2, La_2O_3/CaO and Li/MgO, respectively. The simulation results indicated that the Na-W-Mn/SiO_2 catalyst offers the best performance among all of the catalysts under isothermal mode.

DOI:10.4186/ej.2017.21.3.77

Table 5. Summary of operating condition for catalyst selection study.

Figure	condition		
	GHSV(1/h)	Temperature (K)	CH_4/O_2 ratio
3	18000-30000	993	3.4
4	18000-30000	1173	7.5
5	18000-30000	1173	4.2
6	18000-30000	1173	3.4
7	18000-30000	1073	3.4
8	18000-30000	993	3.4

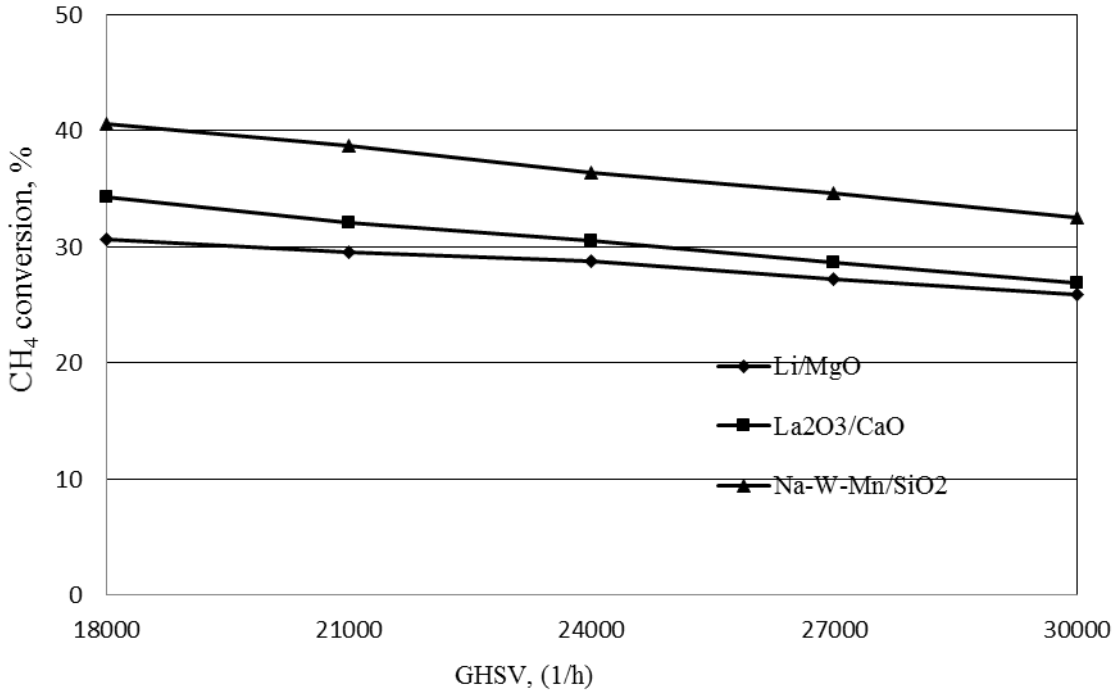

Fig. 3. The activities of Li/MgO, La_2O_3/CaO and Na-W-Mn/SiO_2 catalysts in GHSV range of 18000 to 30000 1/h.

DOI:10.4186/ej.2017.21.3.77

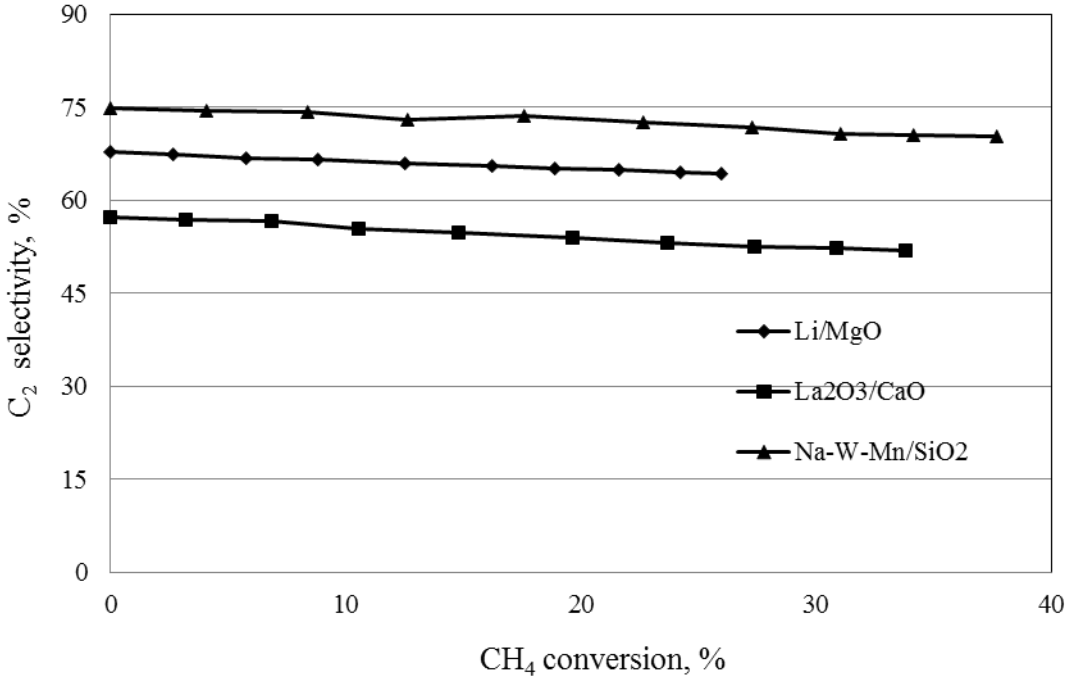

Fig. 4. CH_4 conversion VS C_2 selectivity (T=1173 K, CH_4/O_2 ratio = 7.5).

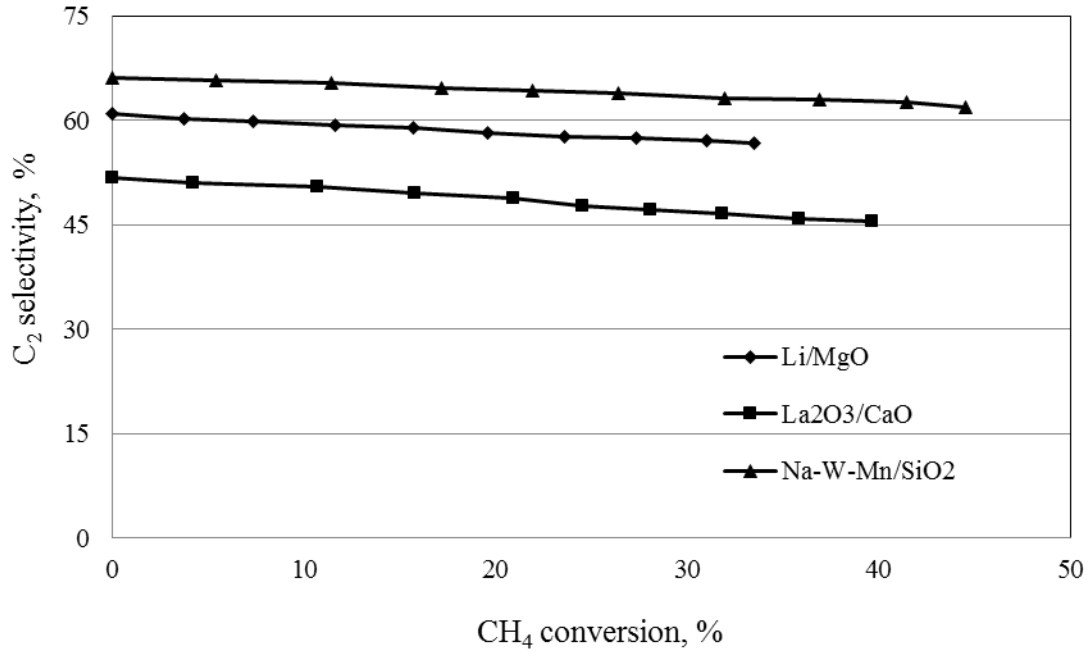

Fig. 5. CH_4 conversion VS C_2 selectivity (T=1173 K, CH_4/O_2 ratio = 4.2).

DOI:10.4186/ej.2017.21.3.77

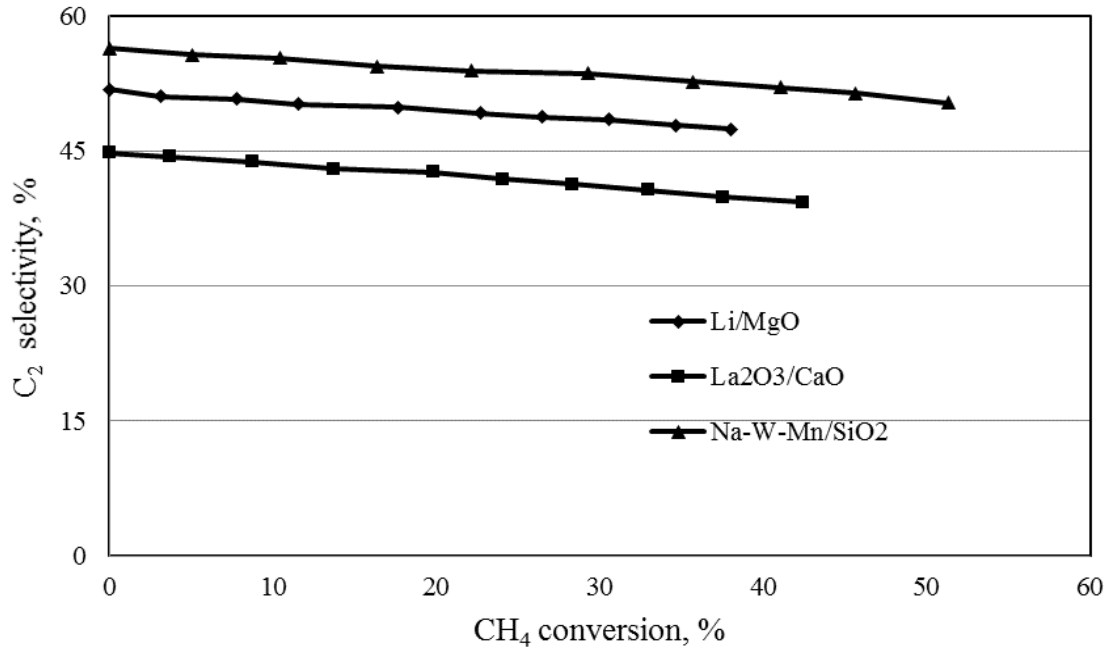

Fig. 6. CH_4 conversion VS C_2 selectivity (T=1173 K, CH_4/O_2 ratio = 3.4).

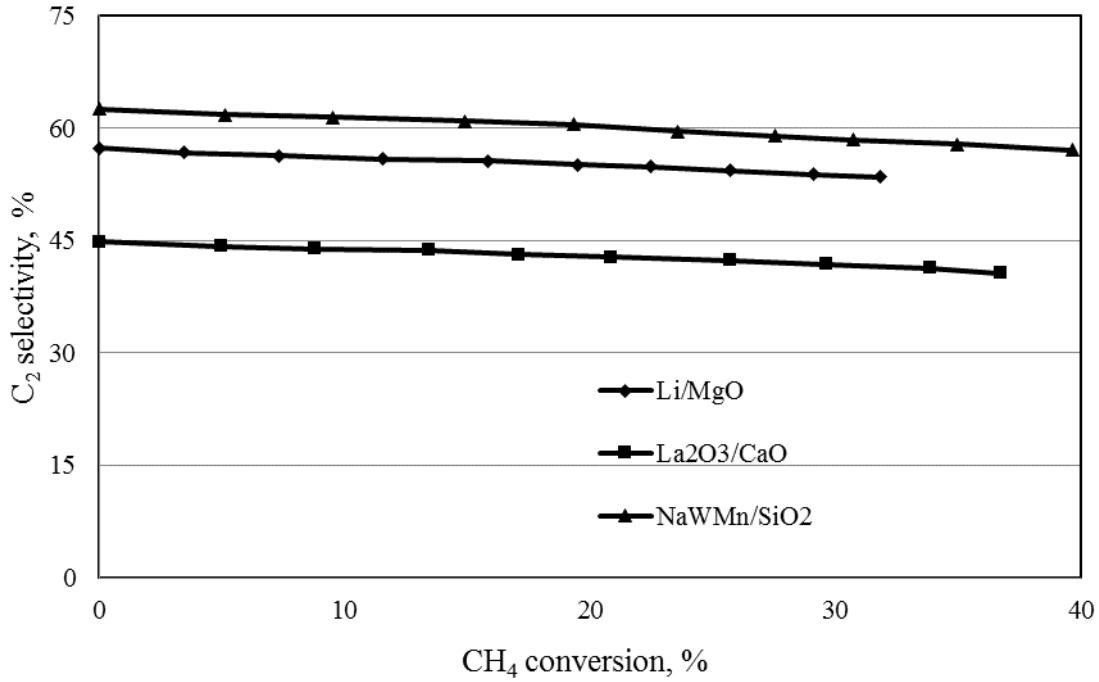

Fig. 7. CH_4 conversion VS C_2 selectivity (T=1073 K, CH_4/O_2 ratio = 3.4).

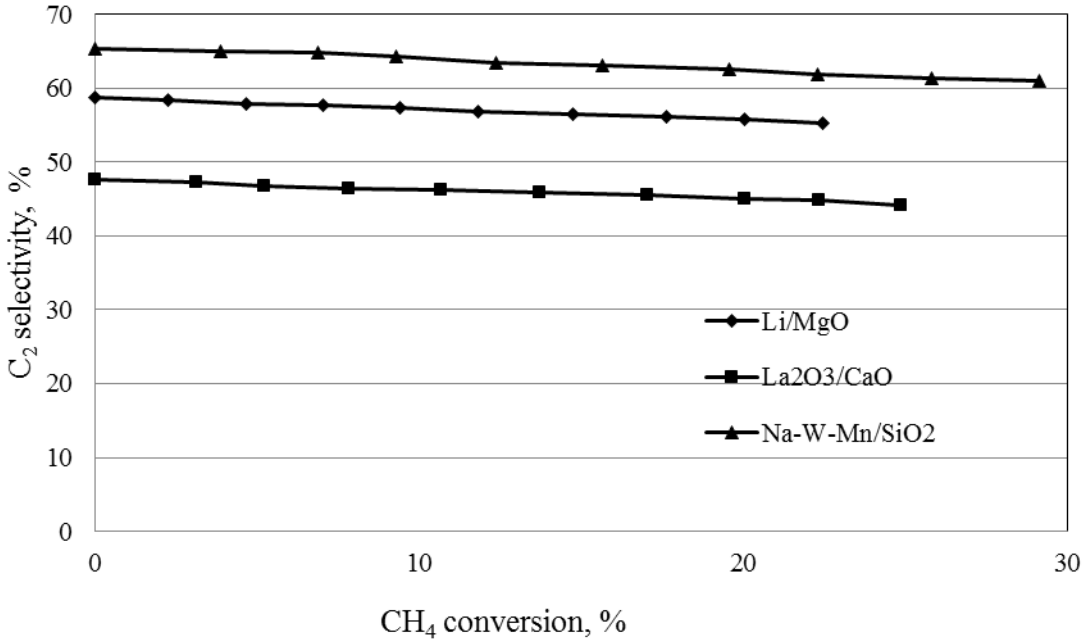

Fig. 8. CH_4 conversion VS C_2 selectivity (T=993 K, CH_4/O_2 ratio = 3.4).

3.3. Fixed Bed Reactor Study

From the previous section, we know that the Na-W-Mn/SiO_2 catalyst exhibits the best performance for the OCM reaction. In the present study, the Na-W-Mn/SiO_2catalyst was selected for this study. The effect of operating conditions, i.e., GHSV, temperature, CH_4/O_2 ratio and air flow rate, was investigated in a fixed bed reactor under non-isothermal mode. The 2-dimensional model was used to explore the profiles of temperature and concentration in the axial and radial directions.

3.3.1. Effect of GHSV

The effect of GHSV in a range of 9000 to 33000 1/h, at a CH_4/O_2 ratio of 2 and at a temperature of 1073 K on the CH_4 conversion and the C_2 selectivity is presented in Fig. 9. The CH_4 conversion decreased, whereas the C_2 selectivity increased with the increase of the GHSV. Increasing the GHSV results in a lower contact time and hence, the CH_4 and O_2 conversions were decreased (Fig. 10 for O_2 conversion). However, the higher GHSV was more favourable for the C_2 hydrocarbon production because the shortening of the contact time between the C_2 products with the oxygen can limit the formation of carbon oxides.

Figure 11 shows the ethylene concentration profile. The GHSV was considered at 9720 (a.), 16197.3 (b.), 25915.7 (c.) and 32394.6 (d.) 1/h, and the temperature and CH_4/O_2 were fixed at 1073 and 2, respectively. From Figs. 11a – 11b, the amount of ethylene was decreased in the middle of a reactor because it reacts with oxygen to form carbon oxides. However, when the GHSV increases, the observed decrease in the amount of ethylene was reduced, as shown in Figs. 11(b)–(d). Figure 12 shows the temperature profile under this condition. For the lower GHSV results (a. and b), dissipation of the hot spot along the axis of the reactor was observed because the OCM reaction and the oxidation of hydrocarbons was highly exothermic. The reactor temperature increases as the reaction heat was accumulated. In this study, the hot spot disappears when operating at high GHSV, as shown in Figs. 12(c)–(d). All of the results indicate that the GHSV has significant influences on both the OCM performance and the thermal management of the reactors.

DOI:10.4186/ej.2017.21.3.77

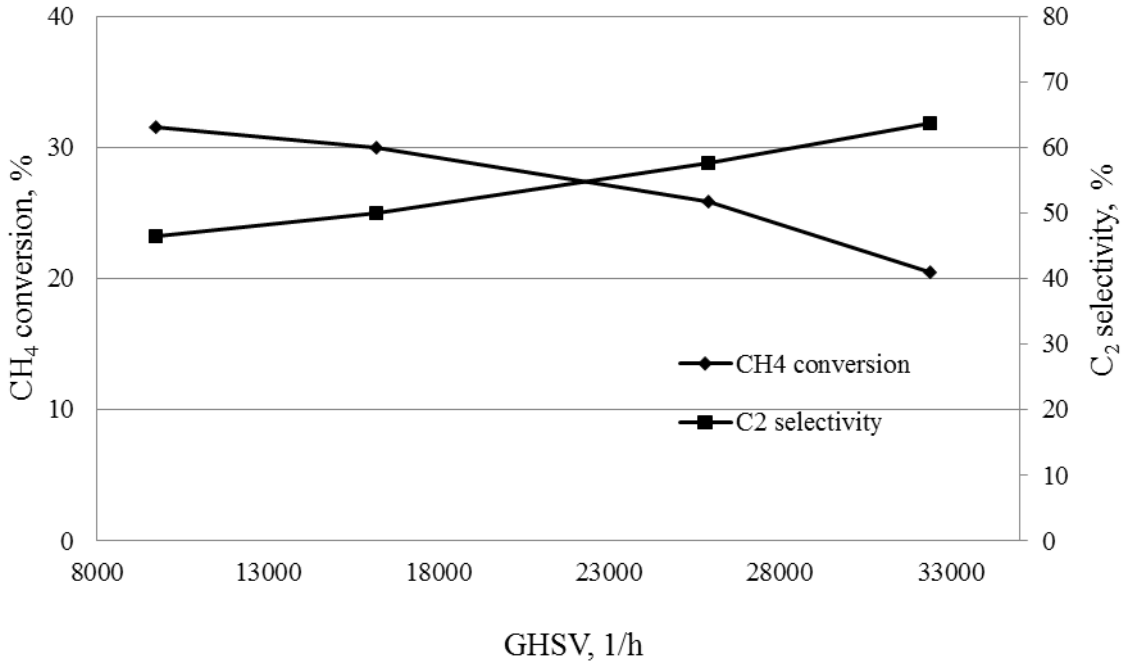

Fig. 9. Effect of GHSV on CH_4 conversion and C_2 selectivity.

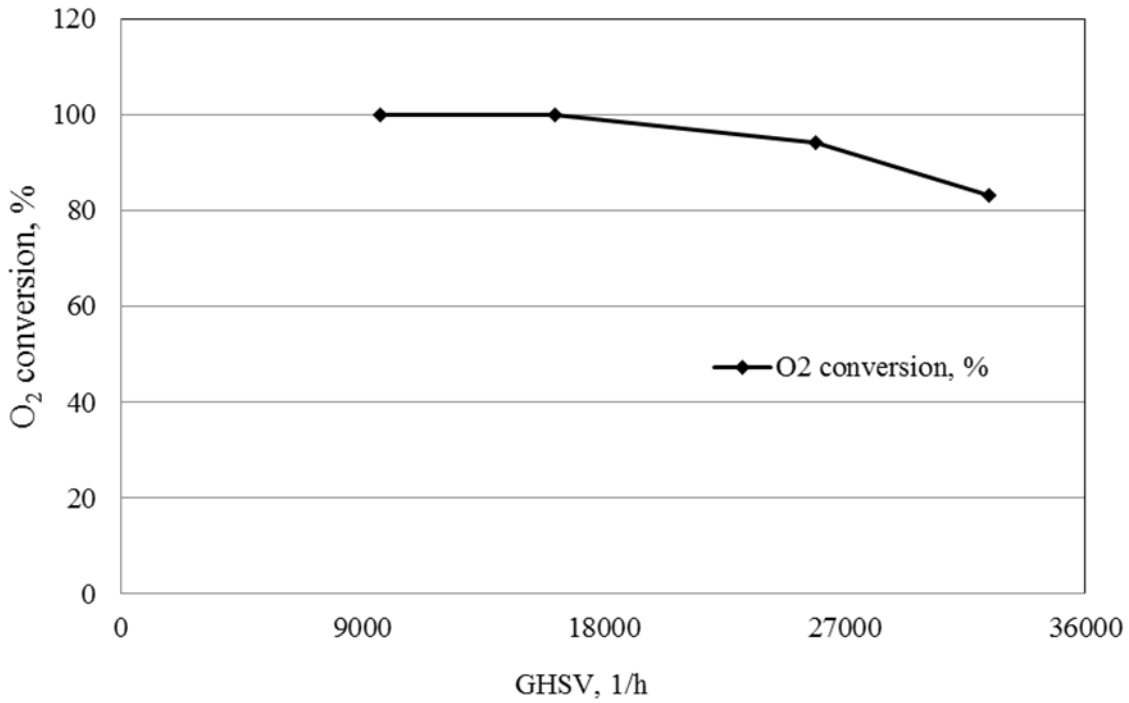

Fig. 10. Effect of GHSV on O_2 conversion.

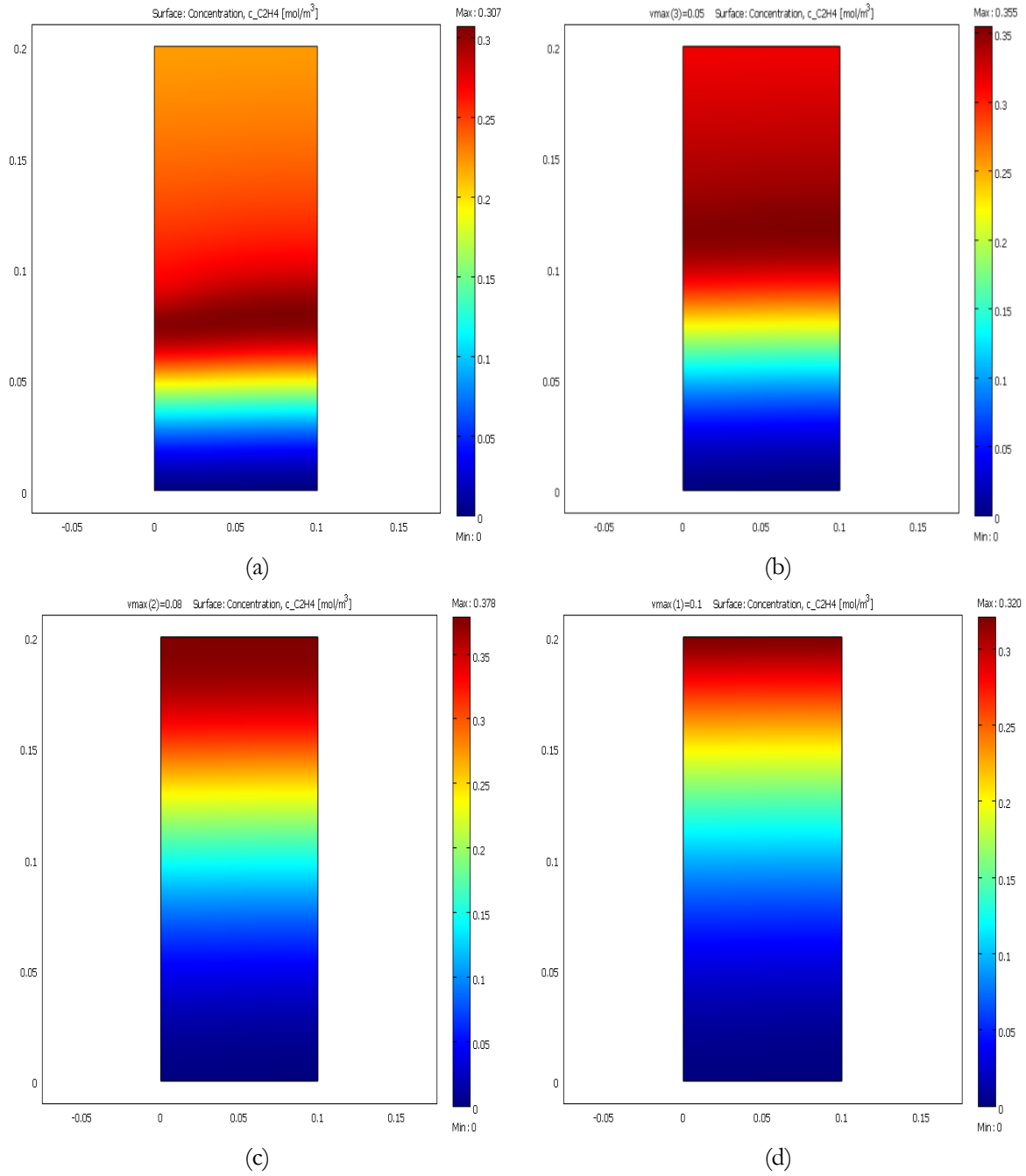

Fig. 11. Effect of GHSV on ethylene concentration profile at 9720 (a.), 16197.3 (b.), 25915.7 (c.) and 32394.6 (d.) 1/h (CH_4/O_2= 2, T= 1073 K).

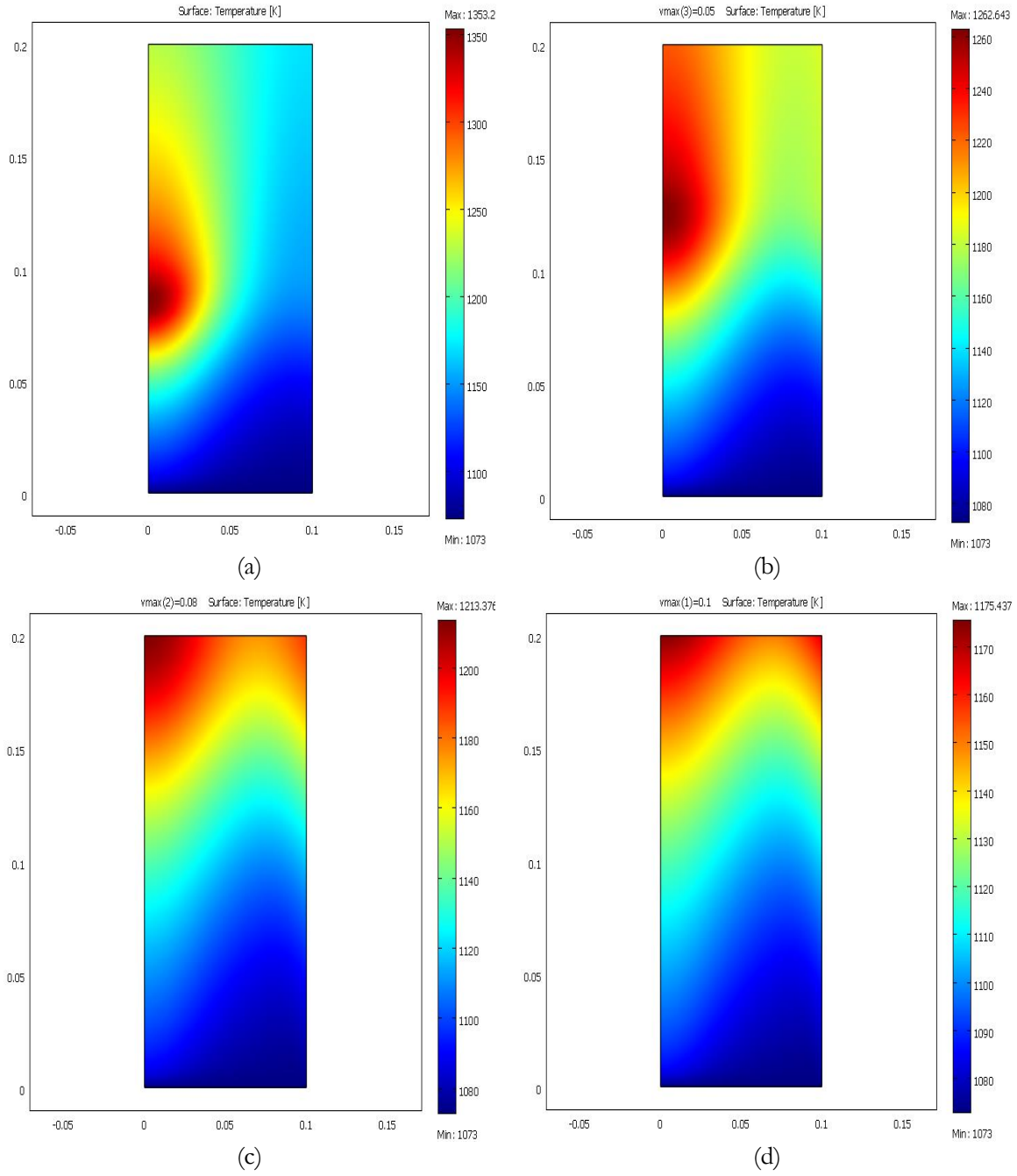

Fig. 12. Effect of GHSV temperature profile (a.), 16197.3 (b.), 25915.7 (c.) and 32394.6 (d.) (CH_4/O_2= 2, *T*= 1073 K).

3.3.2. Effect of temperature

The effect of temperature on the CH_4 conversion and the C_2 selectivity is presented in Fig. 13. The temperature was considered in a range of 993-1173 K, the CH_4 /O_2 ratio was 2 and the GHSV was 9720 1/h. It was found that when increasing the feed temperature, the CH_4 conversion and the CO_x selectivity were increased, thus decreasing the C_2 selectivity. Hence, too high or too low a temperature was not beneficial for the C_2 yield. From the result, the best feed temperature would be 1073 K that represents highest C_2 yields.

Figure 14 shows the temperature profile of the feed temperature at 993 (a.), 1023 (b.), 1073 (c.) and 1123(d.) K, when the CH_4 /O_2 ratio was 2 and the GHSV was 9720 1/h. When increasing the feed

temperature, the maximum temperature was found to increase as well. For the maximum temperature of up to 1543.7 K, the inlet temperature was 1123 K. The heat of reaction released in the OCM increased with the reaction temperature along the reactor. The higher temperature profiles for 1073 K and 1123 K indicate a hot spot occurring along the axis of the reactor. The temperature variation in the radial direction in the same plane lies in the range of 100 to 150 K; hence, safety is a factor that should be considered. The wall temperature was an important parameter, which was related to the heat removal.

These results suggest finding an optimum condition to obtain the best system in this FBR study.

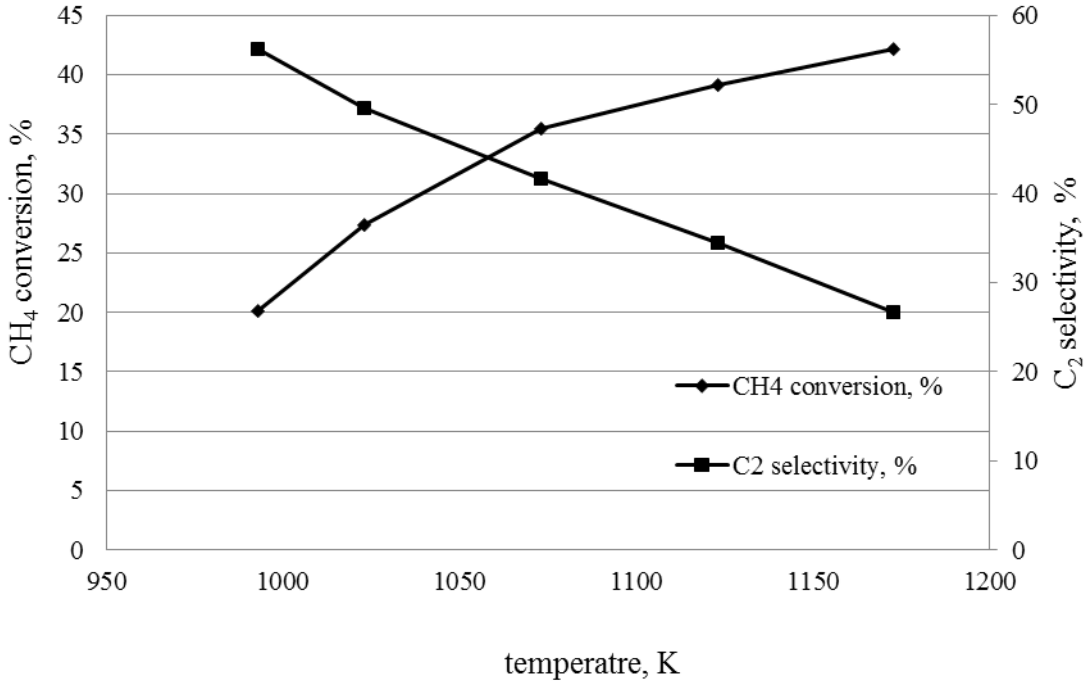

Fig. 13. Effect temperatures on CH_4 conversion and C_2 selectivity.

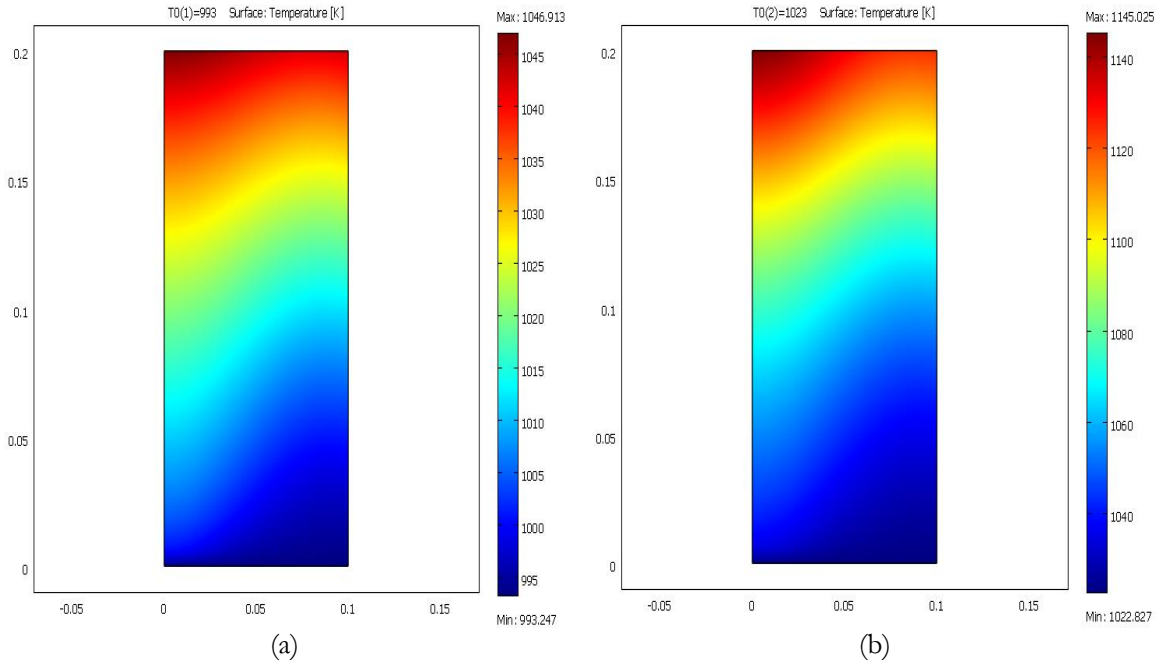

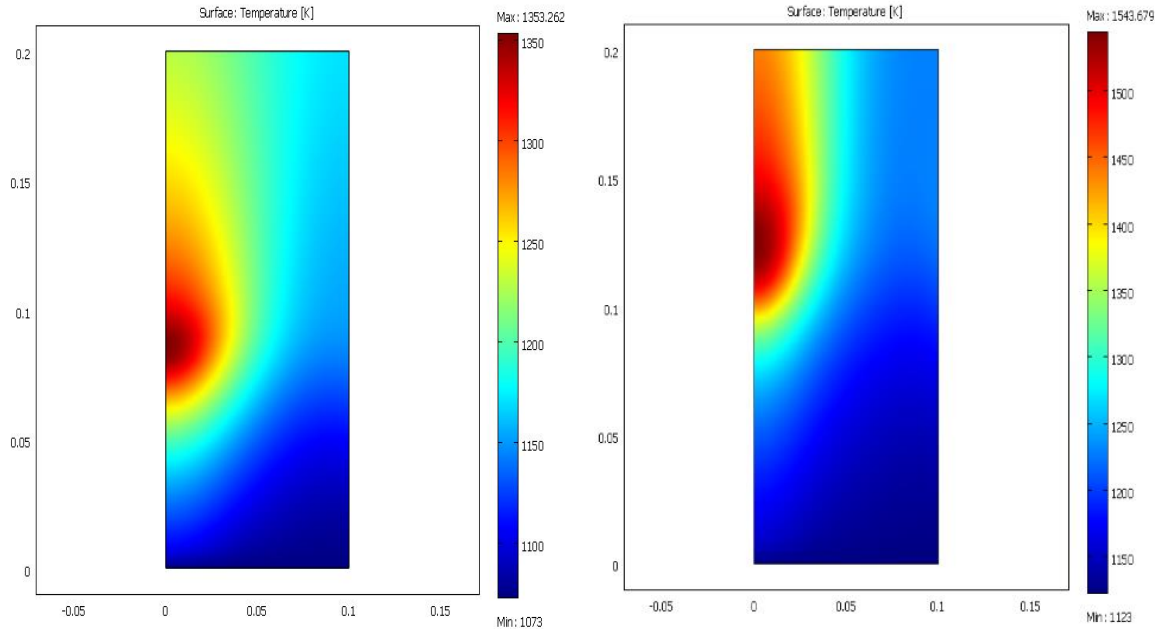

(c) (d)

Fig.14. Temperature profile at T = 993 (a.), 1023 (b.), 1073 (c.) and 1123(d.) K (CH_4/O_2 = 2, GHSV = 9720 1/h).

3.3.3. Effect of CH_4/O_2 ratio

The effect of the CH_4/O_2 ratio in a range 2-7.5 at a GHSV of 9720 1/h and a temperature of 1073 K on the CH_4 conversion and the C_2 selectivity is presented in Fig. 15. The CH_4 conversion was decreased, whereas the C_2 selectivity was increased with the increase of the CH_4/O_2 ratio. The oxygen also causes the production of methyl radicals which cause the formation of C_2 hydrocarbons. Because the oxygen content in feed was decreased to cause an insufficient amount of oxygen in the reaction, the CH_4 conversion was decreased. However, when the oxygen concentration was high (low CH_4/O_2 ratio) the oxidation of methane and the C_2 product became pronounced. Figure 16 shows the oxygen and ethylene concentrations at CH_4/O_2 ratios of 2 and 3.4 in Figs. 16(a) and 16(b), respectively, to provide a comparison on the OCM performance. At a CH_4/O_2 ratio of 2, Fig. 16(a1) shows the O_2 conversion was 100% at the first part of the reactor and that the CH_4 conversion was as high as 55.83 %. In addition, Fig. 16(a2) shows that the ethylene concentration starts to decrease at same point of 100 % conversion of oxygen because it was oxidized to CO_x. The ethylene concentration was improved with increasing CH_4/O_2 ratio to 3.4, as shown in Fig. 16(b). In addition, the effect of the CH_4/O_2 ratio has an influence on the temperature in the reactor. Figure 17 shows the temperature profile at CH_4/O_2 ratios of 2 (a.) and 3.4 (b.). The hot spot disappeared when the CH_4/O_2 ratio was 3.4 because the reaction site is extended along the inner wall thus reaction is faster with higher selectivity and yield, at the same time reducing the hot spot existing in catalyst.

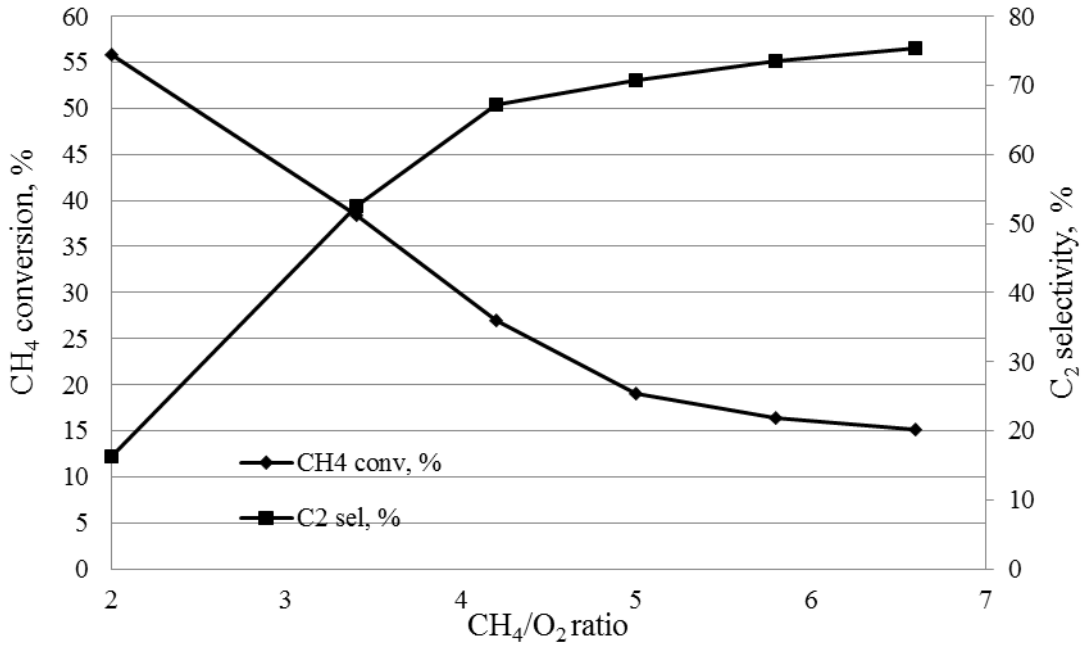

Fig. 15. Effect CH_4/O_2 ratio on CH_4 conversion and C_2 selectivity.

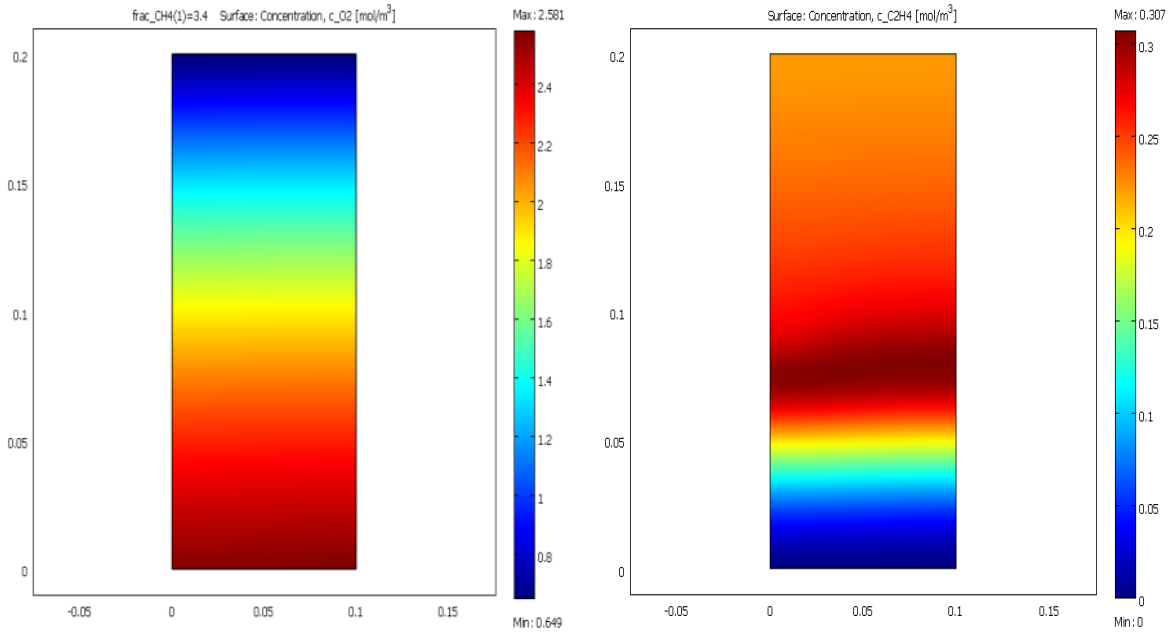

(a1) (a2)

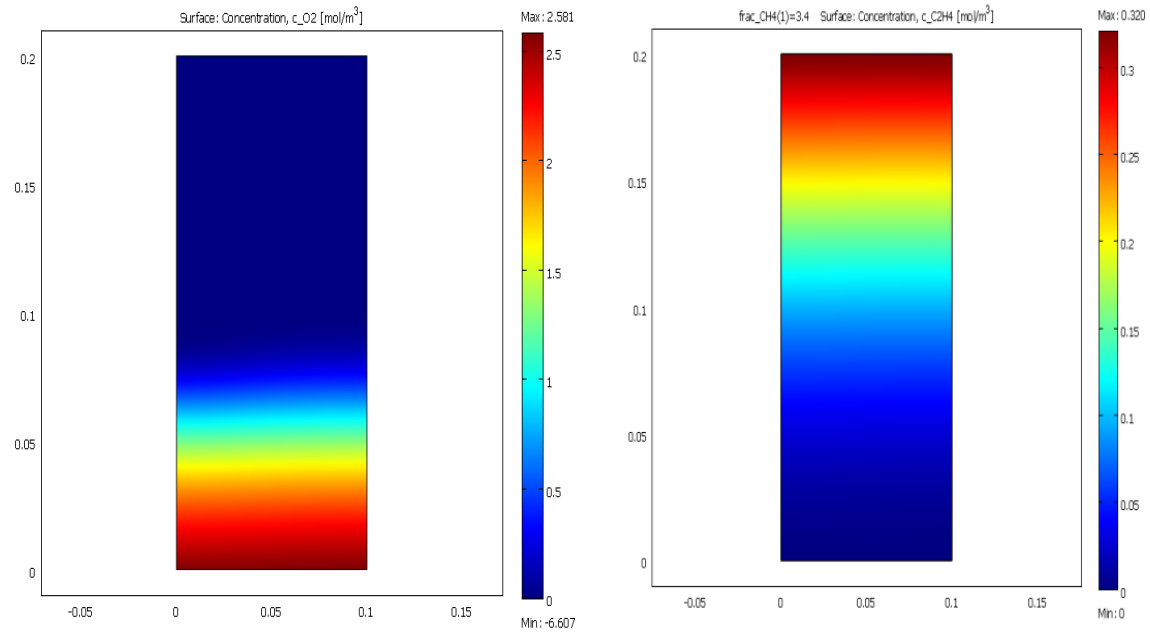

(b1) (b2)

Fig. 16. Effect of CH_4/O_2 ratio on concentration profile a. CH_4:O_2 =2, *T*=1073 K, GHSV =9720 1/h b. CH_4:O_2 =3.4, *T*=1073 K, GHSV =9720 1/h.

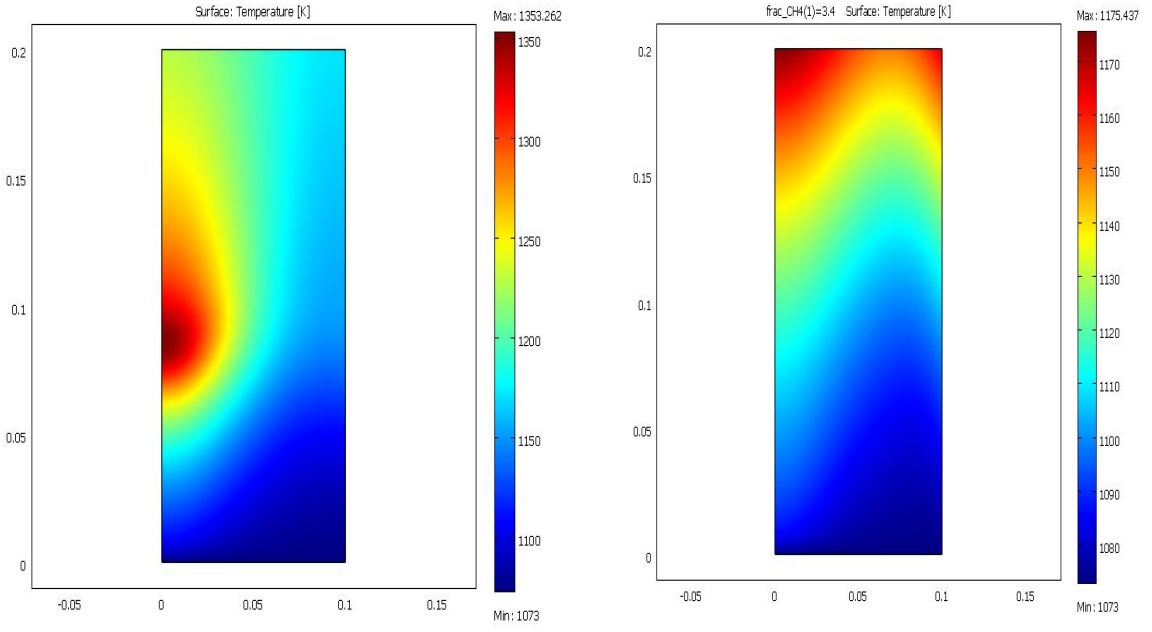

(a) (b)

Fig. 17. Effect of CH_4/O_2 ratio on temperature profile a. CH_4:O_2 =2, *T*=1073 K, GHSV =9720 1/h b. CH_4:O_2 =3.4, *T*=1073 K, GHSV =9720 1/h.

3.4. Effect of the Mode of Operation

It was interesting to compare the effect of the mode of operation, including isothermal, adiabatic and non-isothermal conditions, on the CH_4 conversion, the C_2 selectivity and the C_2 yield. Table 6 presents the results of the comparison under the same feed conditions. The OCM process was simulated under

conditions of a CH_4/O_2 ratio of 3.4, a feed temperature of 1073 K and a GHSV of 9720 1/h. When comparing the different modes, the CH_4 conversion in adiabatic mode was higher than those of the non-isothermal mode and isothermal mode, but it exhibited the least C_2 selectivity. Moreover, operation in adiabatic mode exhibits a hot spot (region) along the axis of the reactor, as seen from the temperature profile in Fig. 18(a). To limit the hot spot, providing some arrangement of cooling around the catalyst bed can control the temperature in the reaction, as demonstrated in the case of the non-isothermal operation mode shown in Fig. 18(b). Other methods were proposed to solve the hot spot problem, such as shortening the catalyst bed or dilution of the first portion of the catalyst bed (Moustafa et al. (2007)). The C_2 yield of 20.16 % was achieved in non-isothermal mode, while they were 20.00 % and 17.62 % for isothermal and adiabatic modes, respectively. The nature of the OCM reaction was highly exothermic. Hence, to achieve this operation condition, a cooling temperature with a high heat transfer coefficient was required.

Table 6. OCM performance at different mode operation.

Performance	isothermal	adiabatic	Non-isothermal
CH_4 Conversion, %	36.14	42.27.	38.43
C_2 Selectivity, %	55.35	41.68	52.46
C_2 Yield, %	20.00	17.62	20.16

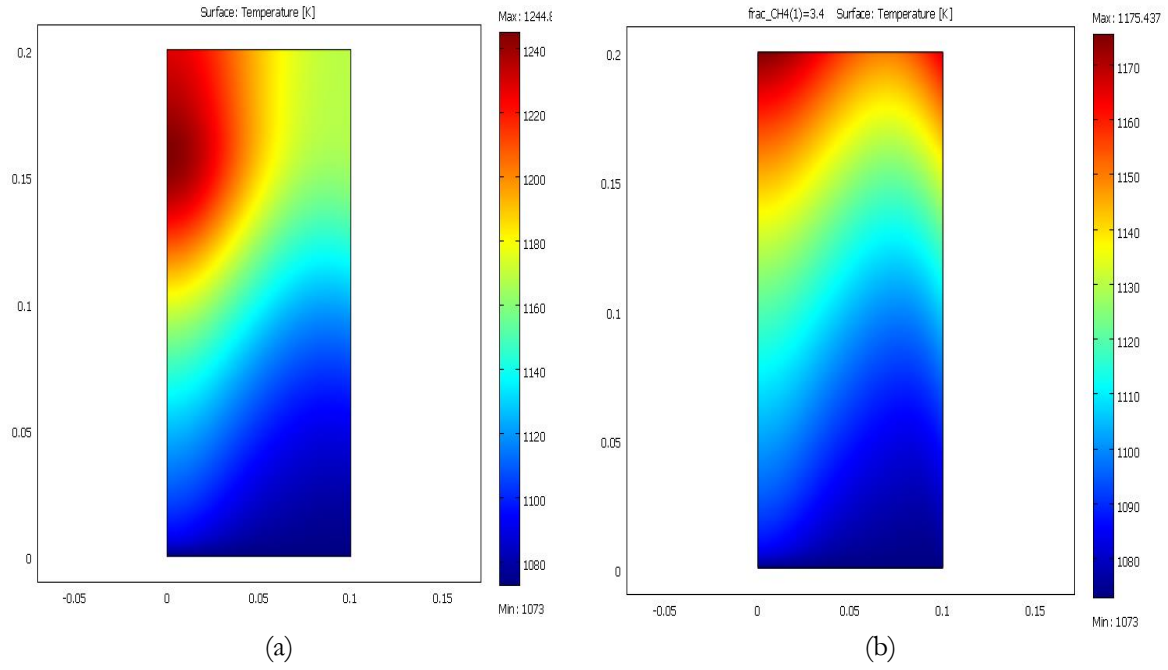

Fig. 18. Effect of mode of operation on temperature profile a. adiabatic mode b. non-isothermal mode (CH_4:O_2 =3.4, *T*=1073 K, GHSV =9720 1/h).

The 2-dimensional model studied and analyzed the effect of operating variables such as CH_4/O_2 ratio, GHSV and temperature in the fixed bed reactor on the reaction performances such as conversion, selectivity, yield via expression of surface plot for each profile (concentration and temperature profiles). The comparison of these results and Karimi *et al.*,2007 supported that the operating condition particularly temperature, GHSV and the CH_4/O_2 ratio was strongly effect the OCM reaction on C_{2+} selectivity, CH_4 conversion and the yield of C_{2+} However the detailed 2D model can provide more accurate predictions of experimental data than the simplified one.

4. Conclusions

Two-dimensional mathematical modeling of the oxidative coupling of methane (OCM) in a fixed bed reactor was studied in this research. The simulations were performed using the Comsol multiphysics program. The present study indicated that the models were well-validated with the previous results reported in the literature. Suitable catalysts were selected via a comparison among the Na-W-Mn/SiO_2, La_2O_3/CaO and Li/MgO catalysts in isothermal mode. The simulation results indicated that the Na-W-Mn/SiO_2 catalyst offers the best performances among all of the catalysts under various conditions. Different operating conditions, such as temperature, CH_4/O_2 ratio and GHSV, influence the performance of the OCM reactors packed with Na-W-Mn/SiO_2 and operated in non-isothermal mode. Increasing the operating temperature increased the CH_4 conversion but decreased the C_2 selectivity However, the effects of CH_4/O_2 ratio and GHSV exhibited contrary results. Especially regarding the hot spots in the reactor, it was found that the three operating variables (CH_4/O_2 ratio, GHSV and temperature) affect the occurrence of hot spots. A suitable condition to achieve the best performance was at a CH_4/O_2 ratio of 3.4, a feed temperature of 1073 K and a GHSV of 9720 1/h. The maximum C_2 yield was 20.16%. In addition, from the studies of the three modes, isothermal, adiabatic and non-isothermal, the results were found for the non-isothermal and isothermal modes; heat management can improve the performance of the OCM reactor, which can be used in a real operation in the reactor design. Moreover, the performance of the OCM may be improved when changing the reactor configuration, e.g., a catalytic membrane reactor should be considered.

Acknowledgements

The authors gratefully acknowledge the Thailand Research Fund (DPG5880003) for the financial support.

References

[1] J. H. Lunsford, "Catalytic conversion of methane to more useful chemical and fuel: A challenge for the 21st century," *Catalysis Today*, vol. 63, pp. 165-174, 2000.

[2] G. E. Keller and M. M. Bhasin, "Synthesis of ethylene via oxidative coupling of methane. I. Determination of active catalysts," *Journal of Catalysis*, vol. 73, pp. 9-19, 1982.

[3] W. Wang and Y. S. Lin, "Analysis of oxidative coupling of methane in dense oxide membrane reactors," *Journal of Membrane Science*, vol. 103, pp. 219-233, 1995.

[4] Z. Stansch, L. Mleczko, and M. Baerns, "Comprehensive kinetics of oxidative coupling of methane over the La_2O_3/CaO catalyst," *Industrial & Engineering Chemistry Research*, vol. 36, pp. 2568-2579, 1997.

[5] S. Lacombe, Z. Durjanova, L. Mleczko, and C. Mirodatos, "Kinetic modeling of the oxidative coupling of methane over lanthanum oxide in connection with mechanistic studies," *Chemical Engineering Technology*, vol. 18, pp. 216–223, 1995.

[6] M. Traykovaa, N. Davidovaa, J. S. Tsaihb, and A. H. Weiss, "Oxidative coupling of methane the transition from reaction to transport control over La_2O_3/MgO catalyst," *Applied Catalysis*, vol. 169, pp. 237-247, 1998.

[7] M. K. S. Shahri and S. M. Alavi, "Kinetic studies of the oxidative coupling of methane over the Mn/Na_2WO_4/SiO_2 catalyst," *Journal of Natural Gas Chemistry*, vol. 18, pp. 25–34, 2009.

[8] S. Kus, M. Otrenba, and M. Taniewski, "The catalytic performance in oxidative coupling of methane and the surface basicity of La_2O_3, Nd_2O_3, ZrO_2, and Nb_2O_5," *Fuel*, vol. 82, pp. 1331–1338, 2003.

[9] S. Pak, P. Qia, and J.H. Lunsford, "Elementary reactions in the Oxidative coupling of methane over Na_2WO_4-Mn/SiO_2 and Na_2WO_4-Mn/SiO_2," *Journal of Catalysis*, vol. 179, pp. 220-230, 1998.

[10] S. J. Li, "Reaction chemistry of W-Mn/SiO_2 catalyst for the oxidative coupling of methane," *Natural Gas Chemistry*, vol. 12, pp. 1-9, 2003.

[11] H. Liu, X. Wang, D., Yung, R. Gao, Z. Wang, and J. Jung, "Scale up and stability test for oxidative coupling of methane over Na_2WO_4-Mn/SiO_2 catalyst in a 200 ml fixed-bed reactor," *Natural Gas Chemistry*, vol. 17, pp. 59-63, 2008.

[12] C. T. Tye, A. R. Mohamed, and S. Bhatia, "Modeling of catalytic reactor for oxidative coupling of methane using La_2O_3/CaO catalyst," *Chemical Engineering Journal*, vol. 87, pp. 49–59, 2002.

[13] Y. K. Kao, L. Lei, and Y. S. Lin, "A comparative simulation study on oxidative coupling of methane in fixed-bed and membrane reactors," *Industrial & Engineering Chemistry Research*, vol. 36, pp. 3583-3593, 1997.
[14] J. H. Lunsford, "The catalytic coupling of methane," *Angewandte Chemie International Edition in English*, vol. 34, pp. 970–980, 2006.
[15] J. A. Langille, J. Pasaleb, J. Y. Renb, F. N. Egolfopoulosa, and T. T. Tsotsisb, "The use of OCM reactors for ignition enhancement of natural gas combustion for practical applications: Reactor design aspects," *Chemical Engineering Science*, vol. 61, pp. 6637-6645, 2006.
[16] N. A. S. Amin and S. E. Pheng, "Influence of process variables and optimization of ethylene yield in oxidative coupling of methane over Li/MgO catalyst," *Chemical Engineering Journal*, vol. 116, pp. 187-195, 2006.
[17] L. Mleczko, U. Pannek, M. Rothaemel, and M. Baerns, "Oxidative coupling of methane over a La_2O_3/CaO catalyst. Optimization of reaction conditions in a bubbling fluidized-bed reactor," *The Canadian Journal of Chemical Engineering*, vol. 74, pp. 279-287, 1996.
[18] M. Daneshpayeh, K. Abbasali, M. Navid, M. Yadolah, S. Rahmate, and T. Alireza, "Kinetic modeling of oxidative coupling of methane over Mn/Na_2WO_4/SiO_2 catalyst," *Fuel Processing Technology*, vol. 90, pp. 403-410, 2009.
[19] S. Bhatia, C. Y. Thien, A. Rahman, "Oxidative coupling of methane (OCM) in a catalytic membrane reactor and comparison of its performance with other catalytic reactors," *Chemical Engineering Journal*, vol. 148, pp. 525–532, 2009.
[20] H. Wang, C. You, and W. Yung, "Oxidative coupling of methane in $Ba_{0.5}Sr_{0.5}Co_{0.8}Fe_{0.2}O_{3-\delta}$ (BSCF) tubular membrane reactors," *Catalysis Today*, vol. 104, pp. 160–167, 2005.
[21] A. Karimi, R. Ahmadi, Z. Bozorg, J. Jebreili, and A. Barkhordarion, "Catalytic oxidative coupling of methane experimental investigation and optimization of operational condition," *Petroleum & Coal*, vol. 49, pp. 36-40, 2007.